An Acad Bras Cienc (2020) 92(4): e20191234 DOI 10.1590/0001-3765202020191234
Anais da Academia Brasileira de Ciências | *Annals of the Brazilian Academy of Sciences*
Printed ISSN 0001-3765 I Online ISSN 1678-2690
www.scielo.br/aabc | www.fb.com/aabcjournal

HEALTH SCIENCES

Gene Expression Profiling in Human Brain Microvascular Endothelial Cells in Response to *Treponema pallidum* Subspecies *pallidum*

FAN WU, KANGJIE SHEN, YI XIE, HONGYE WANG, YIFAN SUN & QIANQIU WANG

Abstract: Neurosyphilis (NS) is a neurological disorder caused by *Treponema pallidum* subspecies *pallidum* (*T. pallidum*), but how *T. pallidum* attach to and cross the blood–brain barrier (BBB) and how BBB response to this bacteria remain unclear. To explore how the human brain microvascular endothelial cells (HBMECs) response to *T. pallidum*, the Agilent SurePrint G3 Human Gene Expression 8×60K microarray was used. The results revealed that 249 genes were differentially expressed in HBMECs infected with *T. pallidum*. In particular, genes encoding proteins involved in bacterial adhesion, endothelial cell activation and immune response were regulated by *T. pallidum*. Furthermore, Gene Ontology (GO) enrichment analysis and Kyoto Encyclopedia of Genes and Genomes (KEGG) analysis were performed to determine the biological functions of differentially expressed genes. In summary, *T. pallidum* changes the gene expression profile in HBMECs, and differentially expressed genes are associated with widespread biological and pathophysiological functions. Above all, this is the first paper reporting the effects of *T. pallidum* on HBMECs. These data develop a new platform for further molecular experiments on the pathogenesis of NS.

Key words: Bacterial adhesion, blood–brain barrier, microarray analysis, scanning electron microscopy, *Treponema pallidum*, vascular endothelium.

INTRODUCTION

Neurosyphilis (NS) is a collective term encompassing a series of severe neurological diseases caused by *Treponema pallidum* subspecies *pallidum* (*T. pallidum*), which is the pathogen of syphilis (Marra 2009). Symptomatic NS is classified into syphilitic meningitis, meningovascular syphilis, general paresis, tabes dorsalis and gumma of the CNS (Ghanem 2010). Recently, there have been increasing reports on NS cases, especially in human immunodeficiency virus (HIV)-positive patients (Farhi & Dupin 2010). Moreover, the clinical manifestations of NS have changed (Chahine et al. 2011), and the misdiagnosis rate of NS is high, and that of neurosyphilitic ischaemic stroke was up to 80.95% (Liu et al. 2012).

T. pallidum have been found in the cerebrospinal fluid of syphilis patients at all stages of infection, which indicates that they can invade the CNS within days of infection (Chung et al. 1994). Clinical studies show that NS patients have abnormal humoral and cellular immunity (Wang et al. 2015, Pastuszczak et al. 2013, Li et al. 2013), and the inflammatory system in the CNS may be activated (Lu et al. 2016). The rabbit model of NS confirmed the existence of neuroinvasive *T. pallidum* strains, and the clinical manifestation of infected rabbits varied with the infecting strains (Tantalo et al. 2005). A scanning electron microscopy study showed that *T. pallidum* could directly attach to cultured nerve cells (Repesh et al. 1982). *T. pallidum* typing studies showed that the preferential strain types of NS were from different areas (Molepo et al. 2006, Marra et al. 2010, Dai et al. 2012). These data suggest that *T. pallidum* has the potential to attach to and cross the blood–brain barrier (BBB), which further causes CNS disorders. However, as an infectious agent, how *T. pallidum* adheres to and across the BBB is largely unknown. In recent years, due to the development of in vitro BBB models based on human brain microvascular endothelial cells (HBMECs), which are the major component of the BBB, the current understanding of the molecular interaction between the BBB and some pathogens has significantly improved (Stins et al. 1994, Greiffenberg et al. 1998, Weksler et al. 2005). Scientists have made great achievements in the identification of ligands and response receptors that are associated with bacterial binding to and invasion of the BBB (Kim 2008, 2010). Unfortunately, so far, little is known about the interaction between *T. pallidum* and the BBB.

The major objective of this study was to explore the response of HBMECs to *T. pallidum* at mRNA level and search meaningful genes for further research. Primary HBMECs were used as an in vitro BBB model, and gene microarray analysis technology was used to analyze the gene expression of HBMECs in response to infection with fresh and virulent *T. pallidum* for a period of 4 h. We further performed Gene Ontology (GO) enrichment analysis and Kyoto Encyclopedia of Genes and Genomes (KEGG) analyze to analyse the biological functions of these differentially expressed genes.

MATERIALS AND METHODS

Ethics statement

Mature male New Zealand White rabbits (n=6) were obtained and housed in a 20°C temperature-controlled room with food and water available *ad libitum* at the China Nanjing Command Institute of Military Medicine. When orchitis was considered to be optimal, the rabbit was sacrificed with an intravenous injection of pentobarbital (90 mg/kg). All surgery was performed under sodium pentobarbital anesthesia, and all efforts were made to minimize suffering. This study was reviewed and approved by the Institutional Animal Care and Use Committee (IACUC) of the Institute of Dermatology, Chinese Academy of Medical Sciences and Peking Union Medical College (Permit Number: 2015-KY024).

Bacterial strains

In the present study, we used *T. pallidum* (Nichols strain). *T. pallidum* was a kind gift from Prof. Tian-Ci Yang, Zhongshan Hospital of Xiamen University, China and was maintained by intratesticular inoculation of rabbits, which were 3 months old and had well-developed testes. *T. pallidum* was passaged and harvested as described previously (Robertson et al. 1982). To remove gross debris and whole cells from the extract, freshly harvested treponemes were centrifuged at 700×g twice for 5 min. The bacterial suspension was centrifuged at 12,000×g for 30 min at 4°C. Then, the supernatant was discarded, and the pelleted treponemes were resuspended in 1 ml fresh cell culture medium. The bacterial suspension was centrifuged at 300×g for 3 min at 4°C again. The supernatant containing treponemes was collected and diluted to an optimal concentration with fresh cell culture medium.

Cell culture and infection

Primary HBMECs (ACBRI 376) were purchased from Cell Systems (Kirkland, WA, U.S.A.), and cultured with the recommended medium (CSC-Complete Medium Kit R, Kirkland, WA, USA). Endothelial cells were used at passages 4-7 in all experiments. HBMECs were seeded onto T25 flasks and cultured in a 5% CO_2 atmosphere at 37°C. When the HBMECs reached confluence, the cells were infected with *T. pallidum* at a ratio of 40:1 (Fig. 1 and 2). Control cells received fresh CSC-Complete medium. After 4 h of co-incubation, the media was removed, and HBMECs were washed with phosphate-buffered saline three times and harvested in TRIzol reagent (Invitrogen, Carlsbad, CA, U.S.A.).

Microarray analysis, GO enrichment analysis, KEGG analysis

We adopted the Agilent SurePrint G3 Human Gene Expression 8×60K microarray (Agilent, Santa Clara, CA, USA) to identify the expression profiling of HBMECs to *T. pallidum*. Total RNA was extracted from HBMECs using TRIzol reagent (Invitrogen, Carlsbad, CA, U.S.A.). A NanoDrop 2000 (Thermo Scientific, Waltham, MA, USA) and a 2100 Bioanalyser (Agilent, Santa Clara, CA, U.SA.) were used to measure the concentration and purity of total RNA and 1% formaldehyde denaturing gel electrophoresis was used to determine the integrity of the RNA. We used the PrimeScript RT reagent Kit (TaKaRa Biotechnology, Otsu, Shiga, Japan) to synthesize and hybridize cDNA according to the manufacturer's recommendations.

For quality control, data summarization and normalization, the GeneSpring software V12 (Agilent, Santa Clara, CA, USA) was used to analyze the array data from 3 biological replicate experiments. Threshold values of ≥2 and ≤−2-fold change and a Benjamini-Hochberg corrected *P*-value of 0.05 were used to select differentially expressed genes. Data were Log2 transformed and median centered by genes using the Adjust Data function of CLUSTER 3.0 software and then further analyzed by a hierarchical clustering approach with average linkage (Eisen et al. 1998). Java Treeview software (Stanford University School of Medicine, Stanford, CA, U.S.A.) was then used to perform tree visualization.

GO analysis and functional annotation of differentially expressed genes were performed on Gene Ontology (www.geneontology.org) and Web Gene Ontology Annotation Plot (WEGO) based on statistical significance, respectively. If the corrected *P*-values were <0.05, the resulting GO terms were considered significant. Pathway analysis was performed based on the latest KEGG database version to determine the biological functions of differentially expressed genes. *P*-values of <0.05 were considered statistically significant.

qRT-PCR verification

Seven genes of interest were validated using a qRT-PCR method. qRT-PCR was performed on a Bio-Rad CFX96 Real-Time PCR system using SYBR Green master mix (SYBR Premix Ex Taq II, TaKaRa Biotechnology). The primer sequences for each gene are listed in Table I. The conditions for PCRs were 95°C for 5 min followed by 40 cycles of 95°C for 30 s and 60°C for 60 s. Each sample was measured three times. The $2^{-\Delta\Delta Ct}$ method was used to calculate the relative fold change of mRNA expression level. Gene expression levels of the target genes were normalized to the β-actin levels. Each experiment was independently performed in triplicate.

Table I. List of primers used for the detection of ADAMTS5, CLDN4, DCN, F3, LDLR, RARRES2, MACF1 and β-actin by SYBR Green PCR.

Gene Symbol		Primer sequence
ADAMTS5	Forward primer Reverse primer	5'-GTAAAGCATTTCCCTATGTGTGAC-3' 5'-TTATTATGCCCACTGAACCCAC-3'
CLDN4	Forward primer Reverse primer	5'-CCCTTCCAAGGACACTAATGAG-3' 5'-CAAAACAGAAACCACAAAGAAGG-3'
DCN	Forward primer Reverse primer	5'-GCTTCTTATTCGGGTGTGAGTC-3' 5'-CTTATAGTTTCCGAGTTGAATGG-3'
F3	Forward primer Reverse primer	5'-TAAGTGCAGGAGACATTGGTATTC-3' 5'-GTCAACCATAGAAGCTTTAAGTACC-3'
LDLR	Forward primer Reverse primer	5'-GTATTTGTTCAGTGACTATTCTCG-3' 5'-CCCAGAAGCCACTCATACATAC-3'
RARRES2	Forward primer Reverse primer	5'-TTCCAGGAGACCAGTGTGGAG-3' 5'-CATTTCCGTTTCCTCCCATTG-3'
MACF1	Forward primer Reverse primer	5'-CCAAAACCCTGTTGAACTAAAG-3' 5'-CCAAATTCAATCCACACCTCTA-3'
β-actin	Forward primer Reverse primer	5'-CAGGCACCAGGGCGTGATGG-3' 5'-CGATGCCGTGCTCGATGGGG-3'

RESULTS

Gene expression profile of HBMECs induced by *T. pallidum*

In the present study, a total of 35,377 different human genes were examined by using the Agilent SurePrint G3 Human Gene Expression 8×60K microarray. We detected 249 differentially expressed genes that included 218 upregulated genes and 31 downregulated genes, among which 93 genes were uncharacterized (Table II). Fig. 3 shows the cluster analysis results.

GO enrichment analysis

To determine the classification and functional annotation of all differentially expressed genes, we identified significantly regulated GO biological process terms using WEGO software (Ye et al. 2006). The differentially expressed genes were annotated and classified into 38 functional groups, and the number of groups in three main categories (biological process, molecular function, and cellular component) was 27, 6, and 5, respectively (Fig. 4). Table III shows the top 10 significant GO terms in detail. The GO analysis results showed that most of the significantly enriched GO terms were involved in the biological process ontology. Other important functional groups included protein binding, extracellular region, extracellular space and extracellular region part.

The KEGG enrichment analysis results showed that only the TGF-beta signaling pathway (ko04350) was identified as likely to be relevant to *T. pallidum* infection. The gene encoding decorin was one of the genes upregulated in this pathway.

Table II. Top differentially expressed genes of HBMECs after infection with *Treponema pallidum* for 4 h.

Gene Symbol	FC^{abs}	Gene or protein description/name	GenBank accession no.
RARRES2	14.04	retinoic acid receptor responder (tazarotene induced) 2	NM_002889
NR4A1	10.30	nuclear receptor subfamily 4, group A, member 1	NM_002135
TMC1	8.14	transmembrane channel-like 1	NM_138691
MYCN	8.12	v-myc myelocytomatosis viral related oncogene, neuroblastoma derived (avian)	NM_005378
OR6B2	8.10	olfactory receptor, family 6, subfamily B, member 2	NM_001005853
ADAMTS5	7.30	ADAM metallopeptidase with thrombospondin type 1 motif, 5	NM_007038
LINC00113	6.94	long intergenic non-protein coding RNA 113	AI796012
DCN	6.49	decorin	NM_001920
GSTA5	6.46	glutathione S-transferase alpha 5	NM_153699
NR4A3	6.32	nuclear receptor subfamily 4, group A, member 3	NM_173200
HLA-DQB1	6.22	major histocompatibility complex, class II, DQ beta 1	NM_001243962
PMCHL1	6.03	pro-melanin-concentrating hormone-like 1, pseudogene	NR_003921
1-Mar	6.01	mitochondrial amidoxime reducing component 1	NM_022746
DKK2	5.97	dickkopf 2 homolog (Xenopus laevis)	NM_014421
HLX	5.77	H2.0-like homeobox	NM_021958
F3	5.46	coagulation factor III (thromboplastin, tissue factor)	NM_001993
SOCS2	5.37	suppressor of cytokine signaling 2	NM_003877
NDRG2	5.25	NDRG family member 2	NM_201535
HLA-DQA1	4.99	major histocompatibility complex, class II, DQ alpha 1	NM_002122
SPRY1	4.93	sprouty homolog 1, antagonist of FGF signaling Drosophila	NM_199327
PMCH	4.91	pro-melanin-concentrating hormone	NM_002674
MESTIT1	4.70	MEST intronic transcript 1, antisense RNA (non-protein coding)	NR_004382
NR4A2	4.59	nuclear receptor subfamily 4, group A, member 2	NM_006186
COL11A2	4.27	collagen, type XI, alpha 2	NM_001163771
IGF1	4.21	insulin-like growth factor 1 (somatomedin C)	NM_000618
MACF1	4.12	microtubule-actin crosslinking factor 1	NM_012090
AREG	4.07	amphiregulin	NM_001657

Table II. Continuation

KLF5	4.05	Kruppel-like factor 5 (intestinal)	NM_001730
GRAMD1B	3.88	GRAM domain containing 1B	NM_020716
DIO2	3.75	deiodinase, iodothyronine, type II	NM_013989
TNNI3	3.75	troponin I type 3 (cardiac)	NM_000363
LINC00494	-11.44	long intergenic non-protein coding RNA 494	NR_026958
FOXS1	-3.34	forkhead box S1	NM_004118
CTAGE10P	-3.34	CTAGE family, member 10, pseudogene	NR_003268
SNORD26	-3.26	small nucleolar RNA, C/D box 26	NR_002564
PON3	-3.21	paraoxonase 3	NM_000940
NIPAL4	-3.02	NIPA-like domain containing 4	NM_001172292
PYHIN1	-2.93	pyrin and HIN domain family, member 1	NM_198930
C1orf110	-2.83	chromosome 1 open reading frame 110	NM_178550
LDLR	-2.77	low density lipoprotein receptor	NM_000527
CLDN4	-2.29	claudin 4	NM_001305
SNORD75	-2.21	small nucleolar RNA, C/D box 75	NR_003941
DLX2	-2.08	distal-less homeobox 2	NM_004405
GZMK	-2.05	granzyme K (granzyme 3; tryptase II)	NM_002104
ENC1	-2.04	ectodermal-neural cortex 1 (with BTB-like domain)	NM_003633
CCIN	-2.04	calicin	NM_005893
SNORA24	-2.00	small nucleolar RNA, H/ACA box 24	NR_002963

FC: fold-change.

Verification of the microarray analysis results by qRT-PCR

Seven differentially expressed genes identified by microarray analysis were selected for validation by qRT-PCR, of which five were upregulated genes: RARRES2, ADAMTS5, F3, MACF1, and DCN and two were downregulated genes: CLDN4 and LDLR. These upregulated or downregulated genes have been reported to have antibacterial activity and are involved in the formation of the cytoskeleton, metabolism and coagulation. The results of the microarray analysis and qRT-PCR are shown in Fig 5. We observed that the results of both analysis methods were highly correlated. Therefore, the technique used in the present study was reliable and accurate. Besides, the differences in fold changes between the microarray analysis results and qRT-PCR results might be due to their different detection methods.

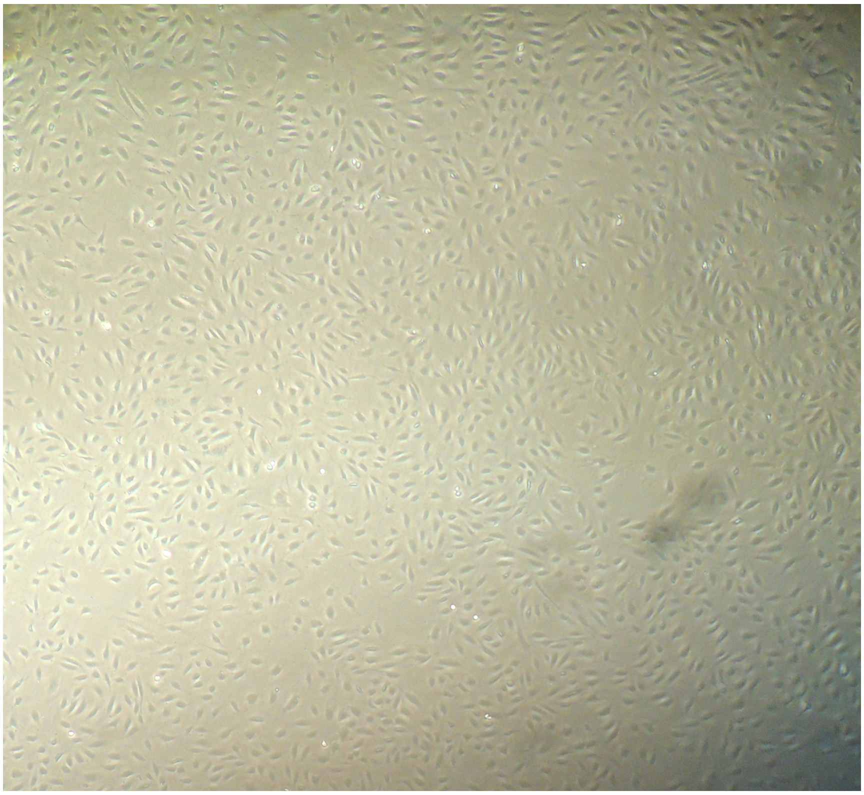

Figure 1. The graph of HBMECs co-incubated with *T. pallidum* with an ordinary optical microscope (400x). We could not see the *T. pallidum*.

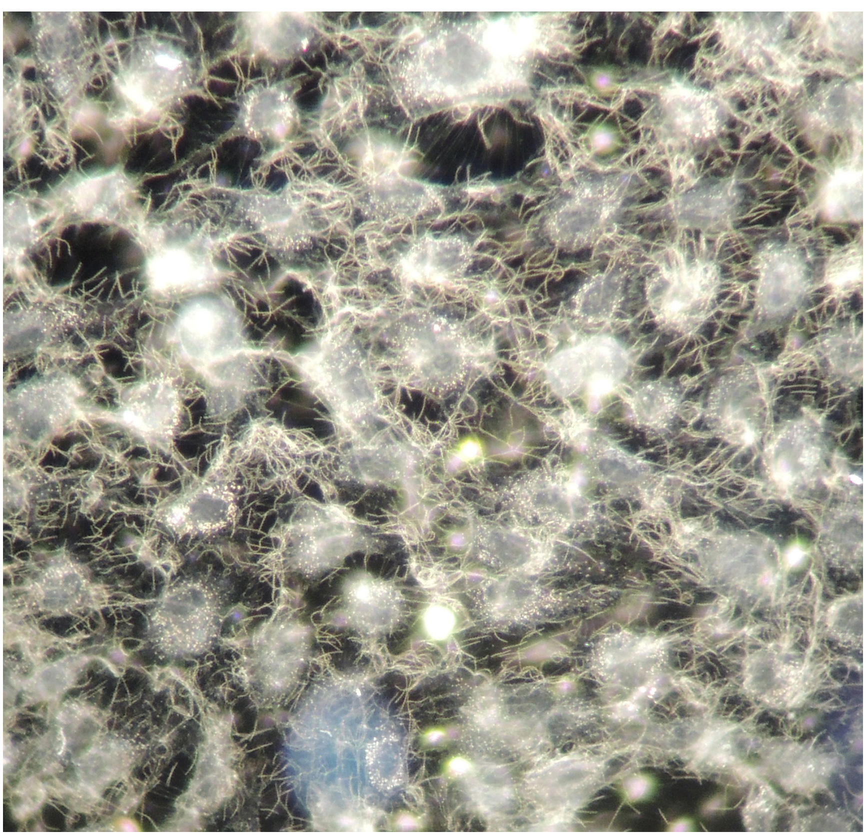

Figure 2. The graph of HBMECs co-incubated with *T. pallidum* with a dark-field microscopy (1000x). We could see *T. pallidum* attached on the HBMECs.

Table III. The top 10 significant GO terms.

GO ID	Term	*P*	Corrected *P*[a]	Gene
GO:0044707	single-multicellular organism process	1.07E-05	0.017713	TLL1,RSPO3,SIK1,RARRES2,SPRY1,DUSP5,DKK2,PBX2,DLX2,OR2H2,STC1,OR10A5,PMCH,DIEXF,NTS,HOXB8,NR4A3,TLL1,ZNF287,INHA,KLF5,TULP2,CCIN,DCN,TNNI3,EPHA7,PER1,SEMA6D,LDLR,BCL2L11,SEMA3A,CRYAB,IGF1,MBP,ENC1,KIF5C,BDNF, OR6B2,F3,NEFM,DGKK,CALCRL,PRRX1,STATH,NLRP3,FOXS1,NR4A2,COL1A1,MRVI1,NR4A1,HOXD9,NDRG2,SHROOM3,CXCL10,HTR1D,JPH1,CSGALNACT1,UNC13C
GO:0005576	extracellular region	1.09E-05	0.002587	TLL1,RSPO3,RARRES2,PZP,CXCL6,DKK2,GZMK,AREG,STC1,PMCH,NTS,TLL1,INHA,TULP2,DCN,IL23A,SELE,LDLR,SEMA3A,IGF1,FREM3,IL1RL1,COL11A2,F3,STATH,COL1A1,CXCL10,PRG4,ADAMTS5,AREG
GO:0005589	collagen type VI	0.00013	0.000129	DCN
GO:0005615	extracellular space	0.000228	0.015793	PZP,DKK2,AREG,STC1,INHA,DCN,IL23A,SELE,LDLR,IGF1,F3,COL1A1,CXCL10,AREG
GO:0044421	extracellular region part	0.000265	0.015793	PZP,DKK2,AREG,STC1,INHA,DCN,IL23A,SELE,LDLR,IGF1,FREM3,COL11A2,F3,COL1A1,CXCL10,ADAMTS5,AREG
GO:0032501	multicellular organismal process	2.05E-05	0.017712	TLL1,RSPO3,SIK1,RARRES2,PZP,SPRY1,DUSP5,DKK2,PBX2,DLX2,OR2H2,STC1,OR10A5,PMCH,DIEXF,NTS,HOXB8,NR4A3,TLL1,ZNF287,INHA,KLF5,TULP2,CCIN,DCN,TNNI3,EPHA7,PER1,SEMA6D,LDLR,BCL2L11,SEMA3A,CRYAB,IGF1,MBP,ENC1,KIF5C,BDNF,OR6B2,F3,NEFM,DGKK,CALCRL,PRRX1,STATH,NLRP3,FOXS1,NR4A2,COL1A1,MRVI1,NR4A1,HOXD9,NDRG2,SHROOM3,CXCL10,HTR1D,JPH1, CSGALNACT1,UNC13C
GO:0007275	multicellular organismal development	2.89E-05	0.017712	TLL1,RSPO3,SIK1,RARRES2,SPRY1,DUSP5,DKK2,PBX2,DLX2,STC1,PMCH,DIEXF,HOXB8,NR4A3,TLL1,ZNF287,INHA,KLF5,CCIN,DCN,TNNI3,EPHA7,SEMA6D,BCL2L11,SEMA3A,CRYAB,IGF1,MBP,ENC1,KIF5C,BDNF,NEFM,CALCRL,PRRX1,FOXS1,NR4A2,COL1A1,NR4A1,HOXD9,NDRG2,SHROOM3,CXCL10,JPH1,CSGALNACT1
GO:0009653	anatomical structure morphogenesis	3.76E-05	0.017712	RSPO3,DUSP5,PBX2,DLX2,HOXB8,NR4A3,KLF5,DCN,TNNI3,EPHA7,SEMA6D,BCL2L11,SEMA3A,CRYAB,IGF1,MYPN,KIF5C,BDNF,CALCRL,PRRX1,FOXS1,NR4A2,COL1A1,NR4A1,SHROOM3,CSGALNACT1

Table III. Continuation

GO:0005515	protein binding	7.62E-05	0.022482	TLL1,RAB27B,RSPO3,CD200,SOCS2,SIK1,RARRES2,SPRY1,BCL2A1,CXCL6,PBX2,STC1,MEF2C,PMCH,NTS,TLL1,DIO2,INHA,DCN,TNNI3,CCRL1,IL23A,EPHA7,SELE,SEMA6D,LDLR,BCL2L11,CRYAB,RRAD,IGF1,DIO2,MYPN,TRIB2,MBP,PFKFB2,ENC1,TRAF1,MYCN,KIF5C,BDNF,IL1RL1,F3,PTCRA,MIA3,NEFM,CALCRL,PRRX1,STATH,NLRP3,FOXS1,NR4A2,LDB2,FEM1A,COL1A1,MRVI1,NFIA,NR4A1,NDRG2,SHROOM3,CXCL10,GPR37L1,CD200,ADAMTS5,DCN
GO:0009605	response to external stimulus	7.5E-05	0.025223	STC1,NR4A3,INHA,DCN,CCRL1,EPHA7,PER1,SEMA6D,LDLR,SEMA3A,KIF5C,BDNF,NR4A2,COL1A1,NR4A1,SHROOM3,CXCL10

GO, gene ontology. [a] Benjamini-Hochberg multiple testing was used for the corrected *P-value*.

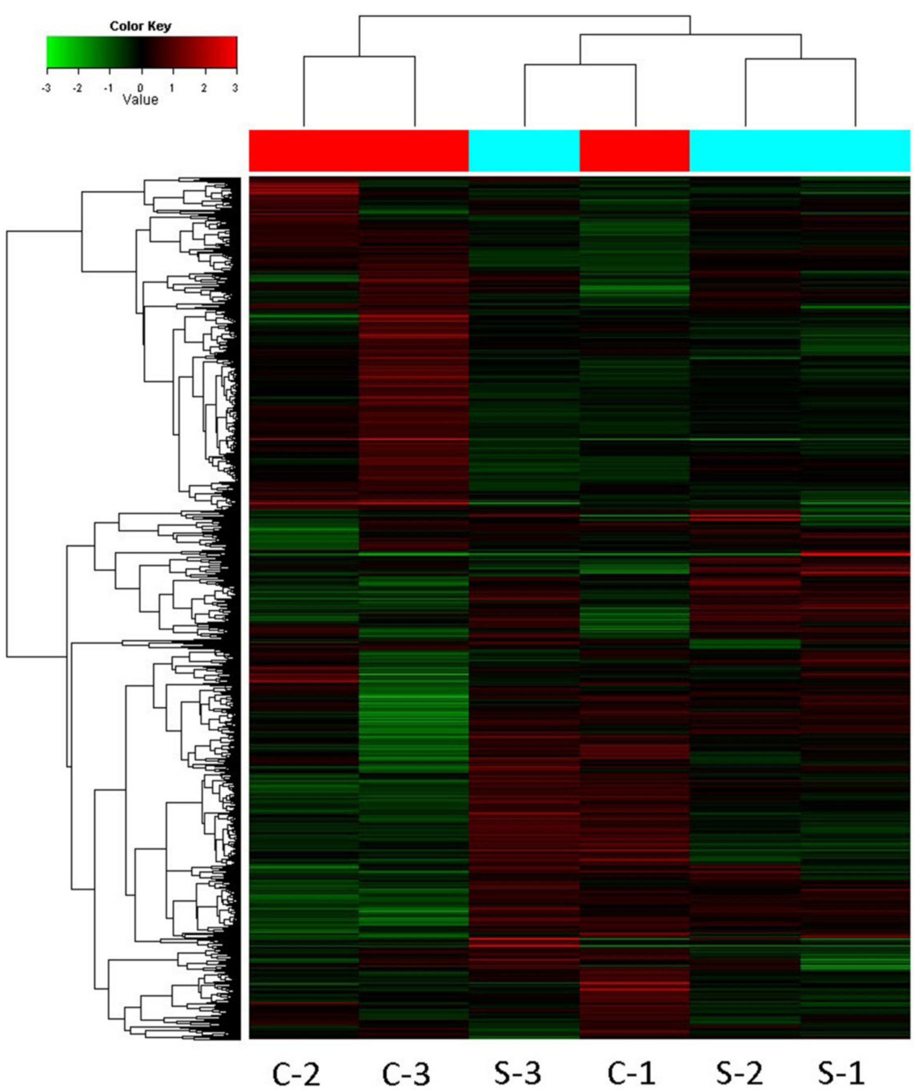

Figure 3. The heat map of differentially expressed genes. Every column represents a sample, and each line represents a single gene. Different colours indicate different expression levels. The red, green and black indicate upregulation, downregulation and no change, respectively. C: control, S: stimulated.

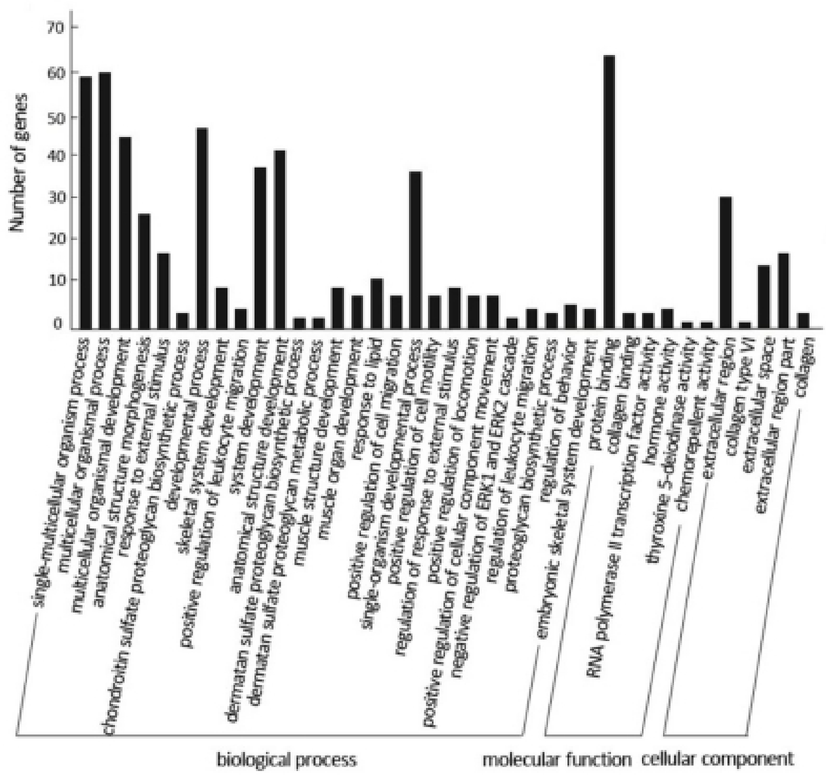

Figure 4. **Gene Ontology (GO) functional annotation. The left-hand Y axis represents the number of genes in the groups.**

DISCUSSION

This is the first study to characterize the gene expression pattern in HBMECs infected with the syphilis-causing pathogen *T. pallidum* based on gene expression microarray analysis technology. A total of 35,377 different human genes were examined in the present study, and significantly differentially expressed genes were observed 4 h post *T. pallidum* infection. This study demonstrated that *T. pallidum* infection induced 249 differentially expressed genes, most of which were upregulated. Further GO analyzed a majority of these significant GO terms classified into the biological process, other important functional groups included protein binding, extracellular region, extracellular space and extracellular region part. The number of differentially expressed genes was significantly less than other mRNA expression profile research of other tumor diseases or inflammatory diseases (Wang et al. 2015, Chen et al. 2015, Guo et al. 2015). The result suggests that the response of HBMECs induced by *T. pallidum* is weakly. The possible reason is that the outer membrane of *T. pallidum* contains a small amount of lipoid and glycoprotein, which may cause a weak immune response to avoid the surveillance of the host immune system. In clinic, patients of NS may be asymptomatic or with mild clinical symptoms.

Similar to other bacteria causing meningitis, *T. pallidum* adhesion to and crossing of HBMECs

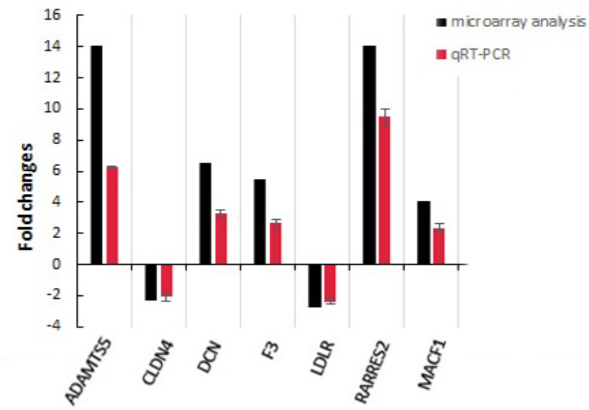

Figure 5. Verification of the microarray results by qRT-PCR. The X-axis shows the seven genes, and the Y-axis represents the fold changes of each transcript. The black bar represents the results of the microarray analysis, and the red bar represents the outcomes of the qRT-PCR. The results of the qRT-PCR are the mean standard deviations (±SD) of at least three replicates.

is a prerequisite for successful disturbance of the CNS. However, until now, there has been no study revealing the interactions between *T. pallidum* and HBMECs. Our results indicated the likely ligands for *T. pallidum* binding to HBMECs for the first time. Among the differentially expressed genes induced by *T. pallidum* infection, we found several genes encoding proteins involved in extracellular matrix, such as decorin (DCN), collagen I and collagen XI. DCN is a small dermatan sulfate proteoglycan that decorates collagen fibers, regulates the production of fibronectin and thrombospondin-1, stimulates collagenase, and inhibits collagen I maturation (Scott & Orford 1981, Zhang et al. 2018). Moreover, DCN is an important ligand for *Borrelia burgdorferi* (*B. burgdorferi*), which is another pathogenic spirochete causing Lyme disease (Guo et al. 1995). Two proteins of *B. burgdorferi* (DbpA and DbpB) have been identified as corresponding adhesins that bind to DCN (Guo et al. 1998). Zambrano *et al.* reported that *B. burgdorferi* can bind to type 1 collagen lattices, but the corresponding adhesion molecule(s) remain unknown (Zambrano et al. 2004). The role of DCN and other collagens in the interaction between *T. pallidum* and HBMECs requires further research.

When endothelial cells are activated by pathogens or related proteins, they may express several kinds of cellular adhesion molecules and open intercellular junctions (Sumitomo et al. 2011). Our results showed that the expression of the gene coding for E-selectin was upregulated and that for claudin-4 was downregulated in infected HBMECs. E-selectin is a marker molecule expressed on the endothelial cell surface, and it plays an important role in the adhesion of leukocytes to the vascular endothelium (Wittchen et al. 2009). Moreover, E-selectin mediates the tethering and rolling of circulating leukocytes on the vascular endothelium during inflammation induced by infection (Kluger 2004). Claudin-4, encoded by *CLDN 4*, belongs to the claudin family, which coordinates with Zonula occluden-1 to maintain endothelial barrier function (Wang et al. 2019). However, how Claudin-4 plays a role in regulating intercellular junctions during bacterial infection is completely unknown. It has been reported that when human umbilical vein endothelial cells (HUVECs) are stimulated by recombinant *Treponema pallidum* protein 0965 (rTp0965), the expression of claudin-1 was decreased (Zhang et al. 2014). Our gene microarray analysis results suggest that HBMECs may be activated in the context of *T. pallidum* binding and invasion, but the details are unclear and require further study in the future.

During microbial invasion, host cells produce a series of immune responses to prevent infection, such as chemokines, cytokines, and oxidative bursts. When HBMECs were infected with *T. pallidum* for 4 h, the expression of genes encoding CXCL-6, CXCL-10, and chemerin were increased. CXCL-6 is a CXC chemokine that exerts neutrophil-activating and angiogenic activities, and the overexpression of CXCL6 can promote the increased expression of pro-angiogenic genes, including IGF-1, VEGF-A, IL-8, and HGF (Kim et al. 2012). Helena et al. demonstrated that CXCL-6 itself was antibacterial, and its antibacterial activity was higher than that of CXCL-5 and CXCL-7 (Linge et al. 2008). Yong et al. also reported that CXCL-6 was significantly elevated in patients infected with some viruses (Yong et al. 2017). CXCL-10, also called interferon γ-induced protein 10 kDa, is another member of the CSC chemokine family and participates in a wide range of physiological and pathophysiology processes, such as chemotaxis, angiostasis, cell growth inhibition and apoptosis. It has been reported that levels of CXCL-10 in body fluids from individuals infected with bacteria, viruses, fungi and parasites are abnormal (Liu et al. 2011). For example, our previous study reported that CXCL-10 was elevated in HBMECs infected with HCV, which might be related to the enrichment of immunocytes (Wu et al. 2018). A study on neuroborreliosis revealed that the gene expression of CXCL-6 and CXCL-10 in HBMECs was significantly upregulated after 72 h of stimulation with *B. burgdorferi* and suggested that neutrophils attracted by chemokines expressed at the BBB may play an important role in the early inflammatory events involved in neuroborreliosis (Brissette et al. 2013). Chemerin is a secreted antimicrobial agent in human skin and is encoded by retinoic acid receptor responder gene 2 (RARRES2) (Banas et al. 2013, Nagpal et al. 1997). Paulina et al. demonstrated that chemerin displayed antibacterial activity against *Escherichia coli* and *Klebsiella pneumonia* and showed bactericidal properties at much lower concentrations (Kulig et al. 2011). Chemerin is also an attractant for leukocytes, including macrophages, dendritic cells, and NK cells, by which chemerin can acquire a pro-inflammatory role (Zabel et al. 2014, Vinci et al. 2012). It is emphasized that the inflammatory response is responsible for syphilis pathogenesis during the invasion and persistence of *T. pallidum*. By recruiting immune cells to sites of tissue damage, vasculitis invokes and ultimately leads to *T. pallidum* dissemination by destroying the endothelial barrier, dependent on the activation of the RhoA/ROCK and MAPK signaling pathways (Zhang et al. 2019). Our previous studies found that recombinant *Treponema pallidum* protein 17 (rTp 17) increased the expression of the gene encoding monocyte chemoattractant protein-1 (MCP-1) in HUVECs (Zhang et al. 2015). Although there is currently no experimental proof, we hypothesize that the chemokines induced by *T. pallidum* may be involved in the interaction between HBMECs and *T. pallidum*, and this hypothesis requires further verification.

In summary, the present study is the first report on global gene expression patterns in HBMECs in response to *T. pallidum*. Our results identified some differentially expressed genes associated with widespread biological processes. More importantly, our research will develop a new platform for further molecular and cellular experiments on the pathogenesis of NS.

Acknowledgments

The authors are grateful to Prof. TianCi Yang for providing the *T. pallidum* Nichols strain and Prof. WuQing Zhou for expert technical assistance. The microarray analysis and qRT-PCR were performed at CapitalBio Corporation, Beijing, China. This study was funded by Natural Science Foundation of Jiangsu Province (BK20190661), the Union Innovation Team Project of the Chinese Academy of Medical Sciences (2016-I2M-3021), the National Natural Science Foundation of China (81772209).

REFERENCES

BANAS M ET AL. 2013. Chemerin is an antimicrobial agent in human epidermis. PLoS ONE 8: e58709.

BRISSETTE CA, KEES ED, BURKE MM, GAULTNEY RA, FLODEN AM & WATT JA. 2013. The multifaceted responses of primary human astrocytes and brain microvascular endothelial cells to the Lyme disease spirochete, Borrelia burgdorferi. ASN Neuro 5: 221-229.

CHAHINE LM, KHORIATY RN, TOMFORD WJ & HUSSAIN MS. 2011. The changing face of neurosyphilis. Int J Stroke 6: 136-143.

CHEN J ET AL. 2015. Screening of differential microRNA expression in gastric signet ring cell carcinoma and gastric adenocarcinoma and target gene prediction. Oncol Rep 33(6): 2963-2971.

CHUNG K, LEE M & LEE J. 1994. Detection of *Treponema pallidum* by polymerase chain reaction in the cerebrospinal fluid of syphilis patients. Yonsei Med J 2: 190-197.

DAI T, LI K, LU H, GU X, WANG Q & ZHOU P. 2012. Molecular typing of *Treponema pallidum*: a 5-year surveillance in Shanghai, China. J Clin Microbiol 50: 3674-3677.

EISEN MB, SPELLMAN PT, BROWN PO & BOTSTEIN D. 1998. Cluster analysis and display of genome-wide expression patterns. Proc Natl Acad Sci U S A 95: 14863-14868.

FARHI D & DUPIN N. 2010. Management of syphilis in the HIV-infected patient: facts and controversies. Clin Dermatol 28: 539-545.

GHANEM KG. 2010. Neurosyphilis: A historical perspective and review. CNS Neurosci Ther 16: e157-168.

GREIFFENBERG L, GOEBEL W, KIM KS, WEIGLEIN I, BUBERT A, ENGELBRECHT F, STINS M & KUHN M. 1998. Interaction of Listeria monocytogenes with human brain microvascular endothelial cells: InlB-dependent invasion, long-term intracellular growth, and spread from macrophages to endothelial cells. Infect Immun 66: 5260-5267.

GUO BP, BROWN EL, DORWARD DW, ROSENBERG LC & HÖÖK M. 1998. Decorin-binding adhesins from Borrelia burgdorferi. Mol Microbiol 30(4): 711-723.

GUO BP, NORRIS SJ, ROSENBERG LC & HÖÖK M. 1995. Adherence of Borrelia burgdorferi to the proteoglycan decorin. Infect Immun 63: 3467-3472.

GUO W, XIE L, ZHAO L & ZHAO YH. 2015. mRNA and microRNA expression profiles of radioresistant NCI-H520 non-small cell lung cancer cells. Mol Med Rep 12(2): 1857-1867.

KIM KS. 2008. Mechanisms of microbial traversal of the blood-brain barrier. Nat Rev Microbiol 6: 625-634.

KIM KS. 2010. Acute bacterial meningitis in infants and children. Lancet Infect Dis 10: 32-42.

KIM SW ET AL. 2012. Mesenchymal stem cells overexpressing GCP-2 improve heart function through enhanced angiogenic properties in a myocardial infarction model. Cardiovasc Res 95(4): 495-506.

KLUGER M. 2004. Vascular endothelial cell adhesion and signaling during leukocyte recruitment. Adv Dermatol 20: 163-201.

KULIG P ET AL. 2011. Regulation of chemerin chemoattractant and antibacterial activity by human cysteine cathepsins. J Immunol 187: 1403-1410.

LI K, WANG C, LU H, GU X, GUAN Z & ZHOU P. 2013. Regulatory T cells in peripheral blood and cerebrospinal fluid of syphilis patients with and without neurological involvement. PLoS Negl Trop Dis 7: e2528.

LINGE HM, COLLIN M, NORDENFELT P, MÖRGELIN M, MALMSTEN M & EGESTEN A. 2008. The human CXC chemokine granulocyte chemotactic protein 2 (GCP-2)/CXCL6 possesses membrane-disrupting properties and is antibacterial. Antimicrob Agents Chemother 52: 2599-2607.

LIU LL, ZHENG WH, TONG ML, LIU GL, ZHANG HL, FU ZG, LIN LR & YANG TC. 2012. Ischemic stroke as a primary symptom of neurosyphilis among HIV-negative emergency patients. J Neurol Sci 317: 35-39.

LIU M, GUO S, HIBBERT JM, JAIN V, SINGH N, WILSON NO & STILES JK. 2011. CXCL10/IP-10 in infectious diseases pathogenesis and potential therapeutic implications. Cytokine Growth Factor Rev 22: 121-130.

LIU Y, CHEN L, ZOU Z, ZHU B, HU Z, ZENG P, WU L & XIONG J. 2016. Hepatitis C virus infection induces elevation of CXCL10 in human brain microvascular endothelial cells. J Med Virol 88(9): 1596-1603.

LU P, ZHENG DC, FANG C, HUANG JM, KE WJ, WANG LY, ZENG WY, ZHENG HP & YANG B. 2016. Cytokines in cerebrospinal fluid of neurosyphilis patients: Identification of Urokinase plasminogen activator using antibody microarrays. J Neuroimmunol 293: 39-44.

MARRA CM. 2009. Update on neurosyphilis. Curr Infect Dis Rep 11: 127-134.

MARRA CM ET AL. 2010. Enhanced molecular typing of *Treponema pallidum*: geographical distribution of strain types and association with neurosyphilis. J Infect Dis 202: 1380-1388.

MOLEPO J, PILLAY A, WEBER B, MORSE SA & HOOSEN AA. 2006. Molecular typing of *Treponema pallidum* strains from patients with neurosyphilis in Pretoria, South Africa. Sex Transm Infect 83: 189-192.

NAGPAL S, PATE LS & JACOBE H. 1997. Tazarotene-induced gene 2 (TIG2), a novel retinoid-responsive gene in skin. J Invest Dermatol 109: 91-95.

PASTUSZCZAK M, JAKIELA B, WIELOWIEYSKA-SZYBINSKA D, JAWOREK AK, ZEMAN J & WOJAS-PELC A. 2013. Elevated cerebrospinal fluid interleukin-17A and interferon-γ levels in early asymptomatic neurosyphilis. Sex Transm Dis 40: 808-812.

REPESH LA, FITZGERALD TJ, OAKES SG & POZOS RS. 1982. Scanning electron microscopy of the attachment of *Treponema pallidum* to nerve cells in vitro. Br J Vener Dis 58: 211-219.

ROBERTSON S, KETTMAN J, MILLER JN & NORGARD MV. 1982. Murine monoclonal antibodies specific for virulent *Treponema pallidum* (Nichols). Infect Immun 36: 1076-1085.

SCOTT JE & ORFORD CR. 1981. Dermatan sulphate-rich proteoglycan associates with rat tail-tendon collagen at the d band in the gap region. Biochem J 197: 213-216.

STINS MF, PRASADARAO NV, IBRIC L, WASS CA, LUCKETT P & KIM KS. 1994. Binding Characteristics of S Fimbriated Escherichia coli to isolated brain microvascular endothelial cells. Am J Pathol 145: 1228-1236.

SUMITOMO T, NAKATA M & HIGASHINO M. 2011. Streptolysin S contributes to group A streptococcal translocation across an epithelial barrier. J Biol Chem 286: 2750-2761.

TANTALO LC, LUKEHART SA & MARRA CM. 2005. *Treponema pallidum* strain-specific differences in neuroinvasion and clinical phenotype in a rabbit model. J Infect Dis 191: 75-80.

VINCI P, BASTONE A, SCHIAREA S, CAPPUZZELLO C, DEL PRETE A, DANDER E, BIONDI A & D'AMICO G. 2012. Mesenchymal stromal cell–secreted chemerin is a novel immunomodulatory molecule driving the migration of ChemR23-expressing cells. Cytotherapy 95(4): 495-506.

WANG C, ZHU L, GAO Z, GUAN Z, LU H, SHI M, GAO Y, XU H, YANG XF & ZHOU P. 2015. Increased interleukin-17 in peripheral blood and cerebrospinal fluid of neurosyphilis patients. PLoS Negl Trop Dis 9: e0003842.

WANG T ET AL. 2015. Transcriptomic profiling of peripheral blood CD4+ T-cells in asthmatics with and without depression. Gene 565(2): 282-287.

WANG X, ZHAO Z, ZHU K, BAO R, MENG Y, BIAN J, WAN X & YANG T. 2019. Effects of CXCL4/CXCR3 on the lipopolysaccharide-induced injury in human umbilical vein endothelial cells. J Cell Physiol 234(12): 22378-22385.

WEKSLER BB ET AL. 2005. Blood-brain barrier-specific properties of a human adult brain endothelial cell line. FASEB J 19: 1872-1874.

WITTCHEN ES. 2009. Endothelial signaling in paracellular and transcellular leukocyte transmigration. Front Biosci (Landmark Ed) 14: 2522-2545.

WU F, HU WL, XU BF & WANG QQ. 2018. Effects of *Treponema pallidum* on the expression of chemokine ligand 6, 8, 10 in human brain microvascular endothelial cells. Chin J Dermatology 51(5): 17-21.

YE J ET AL. 2006. WEGO: a web tool for plotting GO annotations. Nucleic Acids Res 34: W293-297.

YONG YK, TAN HY, JEN SH, SHANKAR EM, NATKUNAM SK, SATHAR J, MANIKAM R & SEKARAN SD. 2017. Aberrant monocyte responses predict and characterize dengue virus infection in individuals with severe disease. J Transl Med 12(1): 121.

ZABEL BA, KWITNIEWSKI M, BANAS M, ZABIEGLO K, MURZYN K & CICHY J. 2014. Chemerin regulation and role in host defense. Am J Clin Exp Immunol 3: 1-19.

ZAMBRANO M, BEKLEMISHEVA A & BRYKSIN A. 2004. Borrelia burgdorferi binds to, invades, and colonizes native type I collagen lattices. Infect Immun 72: 3138-3146.

ZHANG RL, WANG QQ & YANG LJ. 2019. Chemerin induced by *Treponema pallidum* predicted membrane protein Tp0965 mediates the activation of endothelial cell via MAPK signaling pathway. J Cell Biochem July: 1-14.

ZHANG RL, WANG QQ, ZHANG J & YANG LJ. 2015. Tp17 membrane protein of *Treponema pallidum* activates endothelial cells in vitro. Int Immunopharmacol 25: 538-544.

ZHANG RL, ZHANG JP & WANG QQ. 2014. Recombinant *Treponema pallidum* protein Tp0965 activates endothelial cells and increases the permeability of endothelial cell monolayer. PLoS ONE 9: e115134.

ZHANG W, GE Y, CHENG Q, ZHANG Q, FANG L & ZHENG J. 2018. Decorin is a pivotal effector in the extracellular matrix and tumour microenvironment. Oncotarget 9(4): 5480-5491.

How to cite

WU F, SHEN K, XIE Y, WANG H, SUN Y & WANG Q. 2020. Gene Expression Profiling in Human Brain Microvascular Endothelial Cells in Response to *Treponema pallidum* Subspecies *pallidum*. An Acad Bras Cienc 92: e20191234. DOI 10.1590/0001-3765202020191234.

Manuscript received on October 14, 2019;
accepted for publication on February 27, 2020

FAN WU[1]
https://orcid.org/0000-0002-1014-8485

KANGJIE SHEN[2]
https://orcid.org/0000-0002-7281-309X

YI XIE[2]
https://orcid.org/0000-0002-5154-8266

HONGYE WANG[2]
https://orcid.org/0000-0002-6467-0316

YIFAN SUN[2]
https://orcid.org/0000-0002-4205-2103

QIANQIU WANG[3]
https://orcid.org/0000-0003-0654-3826

[1]Department of Dermatology, Sir Run Run Hospital, Nanjing Medical University, No. 109 Longmian Road, Molin District, Nanjing, 211100, China

[2]The First Clinical Medical College of Nanjing Medical University, No. 818 Tianyuandong Road, Molin District, Nanjing, 211100, China

[3]Institute of Dermatology, Chinese Academy of Medical Sciences and Peking Union Medical College, No. 12 Jiangwangmiao Road, Xuanwuhu District, Nanjing, 210042, China

Correspondence to: **Qianqiu Wang**
E-mail: doctorwqq@163.com

Author contributions

Fan Wu and Qianqiu Wang designed experiments; Fan Wu carried out experiments; Kangjie Shen and Yi Xie analyzed experimental results; Hongye Wang and Yifan Sun assisted with Gene Expression microarray; Fan Wu and Qianqiu Wang wrote the manuscript.